

Zhongjian Li,
Ning Zhang,
Yang Wu,
Jing'an Wang,
Ruru Pan,
Weidong Gao*

Evaluation of an Intelligent Computer Method for the Automatic Mosaic of Sequential Slub Yarn Images

DOI: 10.5604/01.3001.0011.5737

Jiangnan University,
Ministry of Education,
Key Laboratory of Eco-textiles,
School of Textiles and Clothing,
Wuxi, Jiangsu, China, 214122
*E-mail: gaowd3@163.com

Abstract

This paper is the second part of a series reporting the recent development of a computerized method for automatic mosaic sequential yarn images. In our earlier work, an effective method for stitching sequence slub yarn images automatically was developed based on image processing and the normalised cross correlation (NCC) method. 100 image pairs of two kinds of slub yarn were measured in certain specific conditions, such as the frame rate, size of stitching template, etc., and the measurement results were evaluated with the manual method. In this paper, the effects of various influencing factors are numerically examined, including the stitching template size, threshold value, frame rate, and computing time of the mosaic algorithm. The feasibility and accuracy of the fully computerized method were evaluated further under the various influencing parameters. One hundred percent cotton ring spun single slub yarns of 27.8, 15.6, and 9.7 tex were prepared and used for the evaluation. The measurement results obtained by the method proposed are analysed and compared with those measured manually by Adobe Photoshop. The experimental results show that the method proposed can accurately find the stitch position and has a high consistency with the manual method when the matching template is $100 \times N$ pixels, the threshold value $T_1 \in [20, 40]$ and $T_2 \in [51, 80]$, and the frame rate is greater than 40 fps.

Key words: sequential slub yarn image; image mosaic, image processing; NCC method.

eters of slub yarn are extremely significant for designing the aesthetic properties of fabric. The traditional method for analysing the slub-yarn parameters is to count slubs in the yarn based on the black boards, which demands special experience from the workers and is a time-consuming and very complicated task for them. Actually in recent research [7-10], the image analysis method seems more appropriate for detecting the parameters of slub-yarn. In these methods, slub yarns are captured by a scanner or area-scan CCD camera. However, the scanning method cannot be used to obtain a sufficient length of slub yarn to analyse the overall performance. Although the area-scan CCD camera method can avoid the disadvantages above, the image captured by this method needs to overlap so as to avert some missing parts of the slub yarn. Thus the image mosaic method has to be employed to seamlessly stitch them together into a panorama for detecting the geometric parameters of slub yarn accurately.

In recent years, a large number of image mosaic algorithms have been applied in many fields, including the speeded up robust feature (SURF) [11], scale invariant feature transform (SIFT) [12] and phase correlation [13]. There is also some existing mosaic software available, such as Panorama Maker [14], Microsoft ICE, Photoshop, and AutoStitch [15]. However, most of the existing methods or

software are only generally suitable for stitching nature images or images with significant features [16].

For the successive yarn images considered in this study, due to the instability of the light source, the intensity values of the same region in different images or different regions in the same image are different. Moreover yarn images are extremely like each other because the yarn core is the largest part in the image, and the operation time of the stitching method required is as little as possible. Therefore the stitching methods or software above cannot be used to splice sequential slub yarn images automatically. In our earlier work [17], an effective method was presented for the automatic mosaic of sequential slub yarn images. After the image acquisition and preprocessing, the normalised cross correlation (NCC) method was utilised to calculate the stitching position, which consists of matching row MR and matching column MC . The two position parameters were employed to evaluate the quality of the image mosaic for each neighboring pair of yarn images. Relative errors E_{MR} and E_{MC} were adopted to evaluate the error of the image mosaic in the vertical and horizontal directions. Another parameter C was employed to assess the consistency of the stitching orientation in the horizontal direction for the manual method and that proposed. 100 image pairs of two kinds of slub yarn were measured

Introduction

Studies of slub yarn are critically important because fabrics woven from them have special aesthetic properties [1-4], which are due to the slub effects formed by the variation in linear density in the slub yarn. The aesthetic characteristics of slub yarn fabric are determined by the apparent parameters of the yarn as fancy yarns have a special structure property [5-6]. Therefore the geometrical param-

in certain specific conditions and the results compared with those of the manual method.

In order to verify the accuracy of the method proposed, the effects of various influencing factors are numerically analysed in this study. Different stitching template sizes, threshold values and frame rates, as well as the computing time, will be discussed in this study to evaluate the image mosaic method proposed. In this paper, one hundred percent cotton ring spun single slub yarns of 27.8, 15.6, and 9.7 tex were prepared and used for evaluation of the automatic mosaic computerised method under the influence of the parameters above. Measurement results of the stitching position obtained by the method proposed are assessed and analysed in comparison to those measured manually by Adobe Photoshop.

In the following analysis, the experimental details, which include sample preparation, image acquisition set-up and the automatic mosaic method proposed in our earlier work, are first described. And then the influential parameters, which consist of the stitching template size, threshold value, frame rate, and computing time, are analysed and discussed in detail to assess the performance of the computerised method in the laboratory experiments. Finally the conclusion is given in the last section.

Experimental details

Sample preparation

In this experiment, 100% cotton ring spun single slub yarns of 27.8, 15.6, and 9.7 tex were used for evaluation of the automatic mosaic method. For each yarn sample, 101 specimens were prepared and tested. Details of the different yarn samples are listed in **Table 1**. In the experiment, stitching position information of all of the slub yarn images will be automatically recognised and measured by the computerised method proposed.

Experimental set-up

The image acquisition set-up is important in capturing a suitable image of the sequence slub yarn. As reported in an earlier study [18, 19], sequence yarn images were taken in succession along the yarn by an area-scan CCD camera with a resolution of 1024×768 pixels. A closed imaging box was used as the image acquisition platform to shield

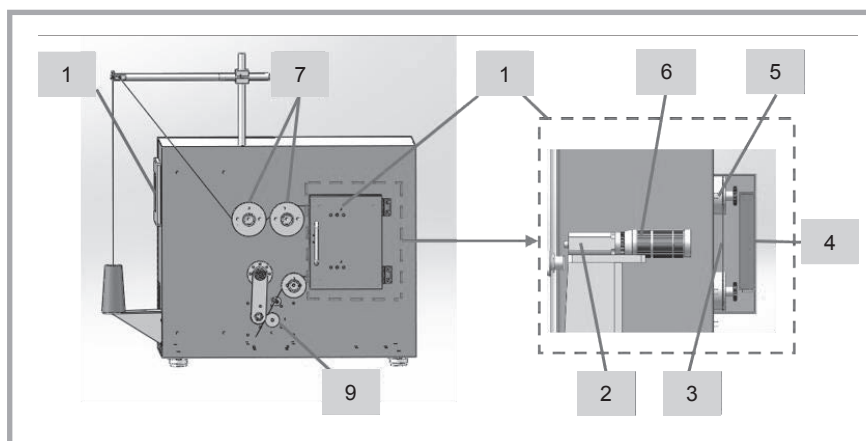


Figure 1. Yarn image acquisition set-up: (1) closed imaging box, (2) area-scan CCD camera sensor, (3) yarn, (4) light source, (5) yarn guiding devices, (6) camera lens, (7) yarn tension control panel, (8) touch screen, (9) output rollers with servo motor.

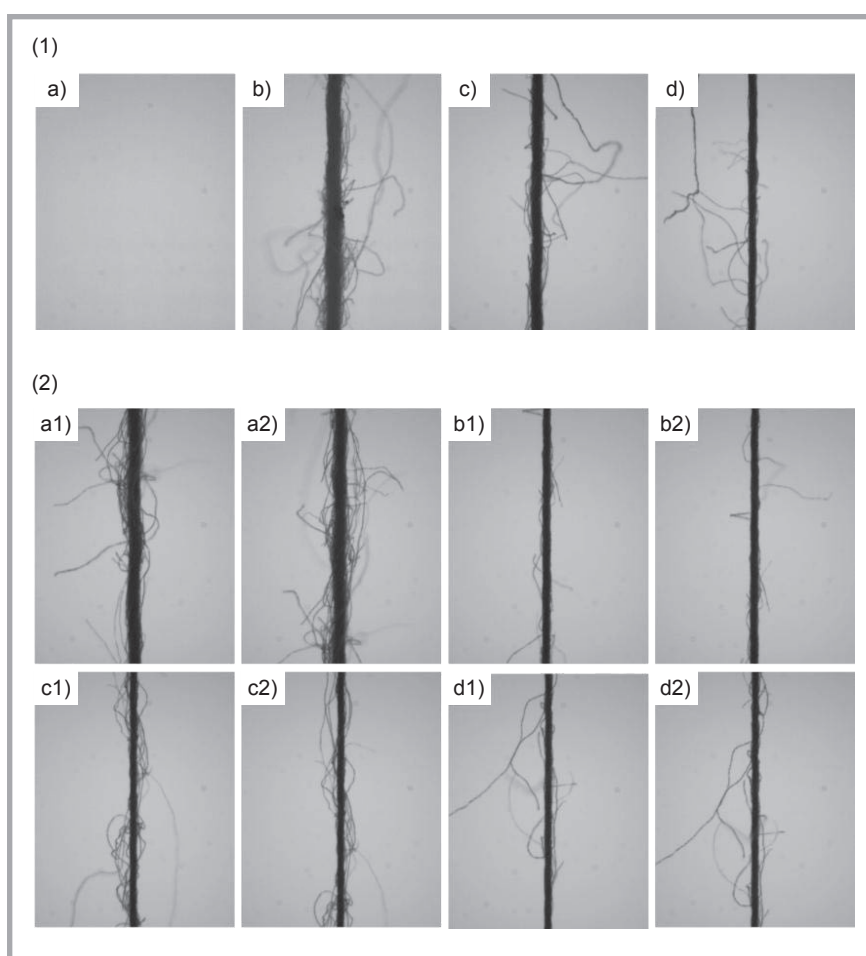


Figure 2. Images captured: (1) background image and three kinds of sub yarn images: a) background image, b) #3 slub yarn – part image of base yarn, c) #2 slub yarn – part image of base yarn, d) #1 slub yarn – part image of base yarn; (2) Image pairs of #1 slub yarn captured at different frame rates: a1)-a2) 40 fps, b1)-b2) 60 fps, c1)-c2) 80 fps, d1)-d2) 100 fps.

Table 1. Three kinds of slub yarn samples.

Sample number	Base yarn count, tex	Spinning method	Material
#1	9.7	Ring spinning	Cotton
#2	15.6	Ring spinning	Cotton
#3	27.8	Ring spinning	Cotton

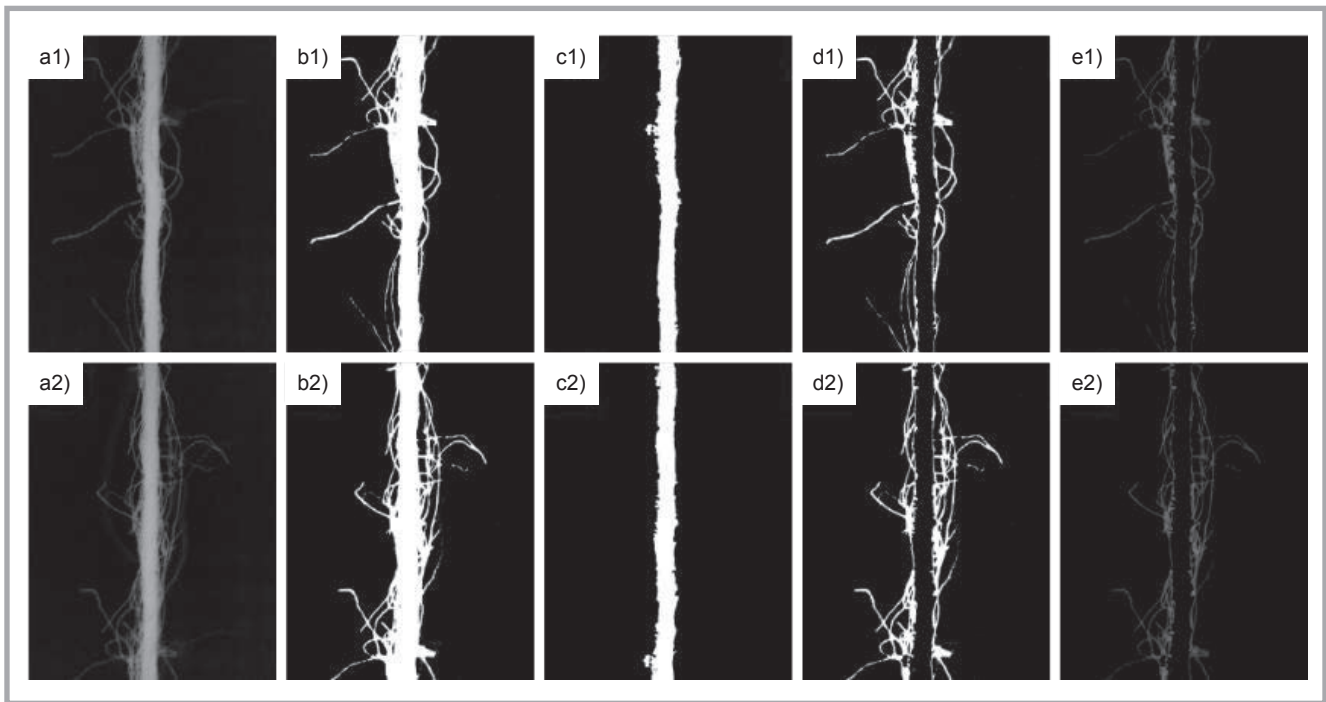


Figure 3. Image processing results of two example images: a1)-a2) image removed background, b1)-b2) binary images with clear hairiness, c1)-c2) yarn core images, d1)-d2) binary-hairiness images, and e1)-e2) gray-hairiness images (TEST 1 and TEST 2 image).

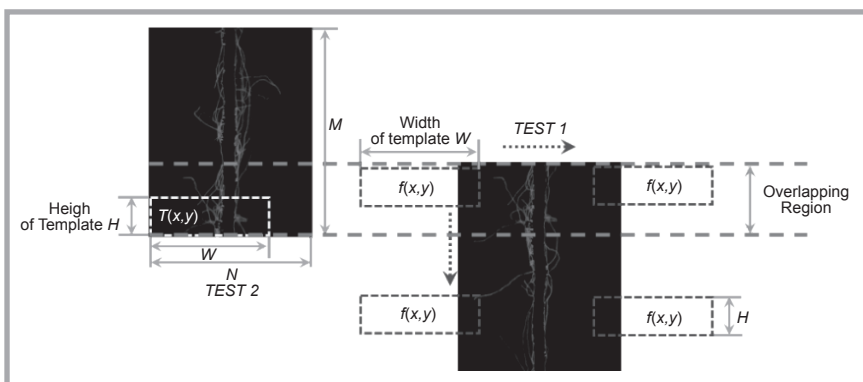


Figure 4. Computation principle of NCC method for yarn image pairs.

the disturbance of ambient light. Meanwhile a special light source was set up in a closed box. A yarn winding mechanism, servo motor, and tension controller were employed to draw the yarn and stabilize the yarn tension. **Figure 1** shows the integrated structure of the image acquisition set-up.

Image acquisition

As shown in **Figure 1**, thousands of slub yarn images can be captured with different frame rates using the image acquisition set-up above, where neighboring images should contain a certain level of overlapping area during acquisition. In this experiment, frame rates of 40, 60, 80 and 100 fps were set to capture the overlap images. The speed of the image acquisition device was uniformly set

at 6 m/min. The background image and three kinds of slub yarn images at four frame rates were captured by the device. These images cropped to a suitable width to allow faster processing are shown in **Figure 2** at the size of 600×768 pixels. According to image calibration, a pixel in the horizontal direction occupies $5.21 \mu\text{m}$ in the image. The real length of yarn in this image is approximately 4 mm.

Image processing and stitching

As reported in our earlier work [17], the procedure of image processing and stitching can be concluded in the following part. Take **Figures 2.a1** and **2.a2** as examples of displaying details of the automatic image mosaic method. The specific steps and results of this method are as follows:

- Remove background information. In this part, the background information is subtracted from all the yarn images to eliminate the impact of non-uniform brightness. The resulting images after background image **Figure 2.a** is subtracted from **Figures 2.a1** and **a.2** are shown in **Figures 3.a1** and **a.2**.
- Segment the resulting images above and extract the yarn core images. In this part, two threshold values T_1 , T_2 and judgment template traversal are applied to process the sequential images to obtain binary images, as shown in **Figures 3.b1-3.b2** and **3.c1-3.c2**. A threshold value T_1 is set to get the first binary image which has clear hairiness (**Figures 3.b1** and **3.b2**). Another threshold value T_2 is applied to segment the original image to obtain a second binary image which has less hairiness. Subsequently two judgment templates are used to remove the little hairiness from the second binary image to obtain yarn core images (**Figures 3.c1** and **3.c2**).
- Eliminate the yarn core from the binary image and execute dot multiplication to obtain a test image (TEST image). The resulting images of **Figure 3.b1** minus **Figure 3.c1** and **Figure 3.b2** minus **Figure 3.c2** are shown in **Figures 3.d1** and **3.d2**. TEST images of **Figures 3.d1**, **3.d2** dot multiplication of the original images (**Figures 2.a1**

and 2.a2) are shown in *Figures 3.e1* and *3.e2*, respectively.

- The NCC method is applied to calculate the stitch position between *TEST 1* image and *TEST 2* image. A specific matrix T with a size of $H \times W$ ($H = 1, 2 \dots M$, $W = 1, 2 \dots N$, M and N are the height and width of the original image) in the *TEST 2* image is selected as the calculated template, as shown in *Figure 4*. H and W are two adjustable parameters which represent the height and width of the template, respectively. Let $T(x, y)$ be the intensity value of T at pixel (x, y) , and $f(x, y)$ be the intensity value of f at pixel (x, y) . f is a movement matrix in *TEST 1* image, whose size is as same as T . The NCC method is evaluated at every point (u, v) for f and T , which has been shifted over the *TEST 1* image by u -steps in the x -direction and v -steps in the y -direction. If the matrix f just consists of a part of the intensity value of the *TEST 1* image (shown as blue rectangles in *Figure 4*), the remaining parts in matrix f are zero-filled. All the NCC coefficients are stored in a correlation matrix $\gamma(u, v)$ as defined by [20-22] *Equation (1)*.

Where \bar{T} is the mean of the template, and $\bar{f}_{u,v}$ that of $f(x, y)$ in the region under the template. These can be defined as:

$$\bar{f}_{u,v} = \frac{1}{H \times W} \sum_{x=1}^H \sum_{y=1}^W f(u-x, v-y) \quad (2)$$

$$\bar{T} = \frac{1}{H \times W} \sum_{x=1}^H \sum_{y=1}^W T(x, y) \quad (3)$$

Here if $u-x < 0$ or $v-y < 0$ then $f(u-x, v-y) = 0$, and $f(0, 0) = \text{TEST 1}(1, 1)$, $f(0, 1) = \text{TEST 1}(1, 2)$, and so on.

In this example, we set $H = 100$ pixels and $W = N$. After the calculation, the matrix $\gamma(u, v)$ is obtained as shown in *Figure 5.a*. In the figure, there is a quite distinct peak at point **P**, denoting that the position of point **P** is the optimum matching position of the two adjacent yarn images. Suppose the position of point **P** is (u_p, v_p) , then the matching position in

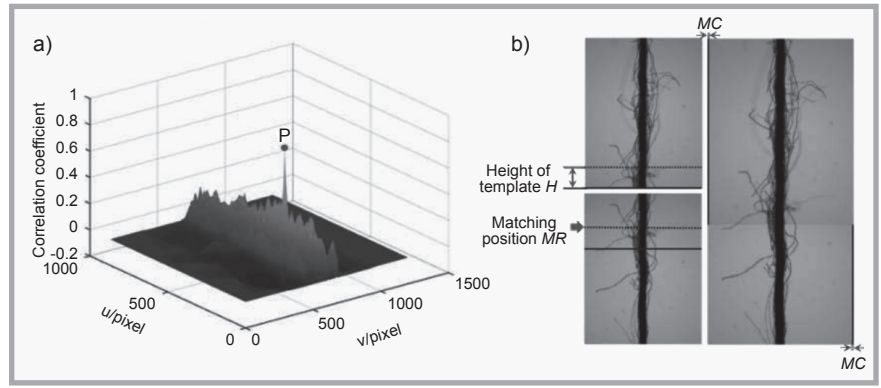


Figure 5. Stitch position information and mosaic result of two TEST images.

the *TEST 1* image, that is, the matching row MR and matching column MC in the *TEST 1* image, can be calculated as:

$$MR = u_p - H \quad (4)$$

$$MC = v_p - W \quad (5)$$

MR and MC are adopted to find the overlapping line between two adjacent yarn images for stitching the yarn images. Finally the original image of *TEST 1* is separated based on MR and MC , and the panoramic image is obtained as shown in *Figure 5.b*, in which the black regions, which represent the width of MC , are located in the bottom right corner and top left corner of the panoramic image. It means that MC is a positive value. Conversely MC is a negative value.

Parameter discussion and data analysis

In our earlier work [17], the accuracy of the image stitch was discussed when the template size was set to $100 \times N$ pixels and the frame rate to 40 fps. In this part, the influence of a different template size, segment threshold value and frame rate on the precision of stitch results are analysed. The computation time is also compared with the manual method. 101 sequence images of three kinds of slub yarn were used to assess the effect under different parameters, and Adobe Photoshop CS2 software was also applied to stitch the yarn images for comparing with the method proposed.

Template size

In order to analyse the influence of different template sizes on the accuracy of yarn image matching and determine the optimal size of the template, the template height H is set from 1 pixel to M (the height of the sequence image) pixels by step 1 pixel. In this paper, the width of template W is set equal to N (the width of the sequence image) because the template cannot be a zero matrix based on the NCC method and must include yarn hairiness information. This can guarantee the maximum level of inspection accuracy. Take the result in *Figure 5.b* as an example, the influence of a different template height can be concluded in *Figure 6*. Here the image pairs are captured at 40 fps. *Figure 6.a* and *6.b* denote the different MR values and various u_p values ($u_p = MR + H$) when using different template heights H to match the next image based on the automatic method proposed and the manual method.

From *Figure 6.a* it can be seen that the MR values are similar for both methods at different template heights. They all decrease with the increasing of the template height H . It seems that the height of template H from 1 to M pixels can all be utilised to match the next image, and it can have a good result. However, there are some negative values of MR in this figure. It means the template height H is greater than the height of the total overlap region between the two *TEST* imag-

$$\gamma(u, v) = \frac{\sum_{x=1}^M \sum_{y=1}^N [T(x, y) - \bar{T}] [\bar{f}_{u,v} - f(u-x, v-y)]}{\left\{ \sum_{x=1}^M \sum_{y=1}^N [T(x, y) - \bar{T}]^2 \times \sum_{x=1}^M \sum_{y=1}^N [f(u-x, v-y) - \bar{f}_{u,v}]^2 \right\}^{0.5}} \quad \begin{matrix} u \in (1, 2, \dots, M + H - 1) \\ v \in (1, 2, \dots, N + N - 1) \end{matrix} \quad (1)$$

Equation (1).

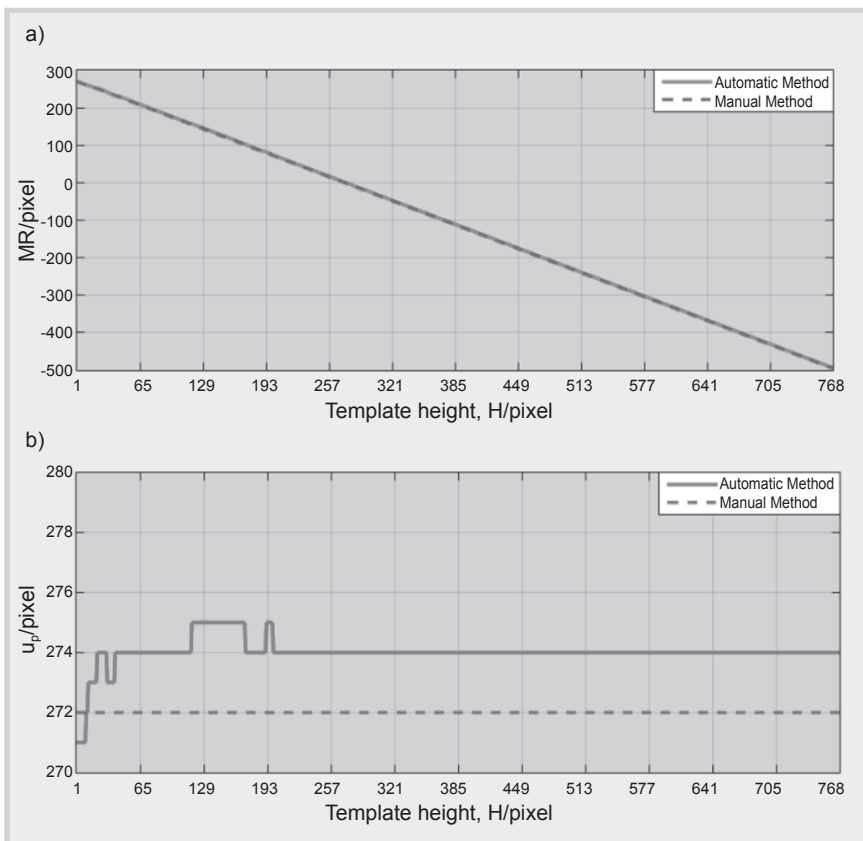


Figure 6. Different MR and u_p values at different template heights based on two calculating methods.

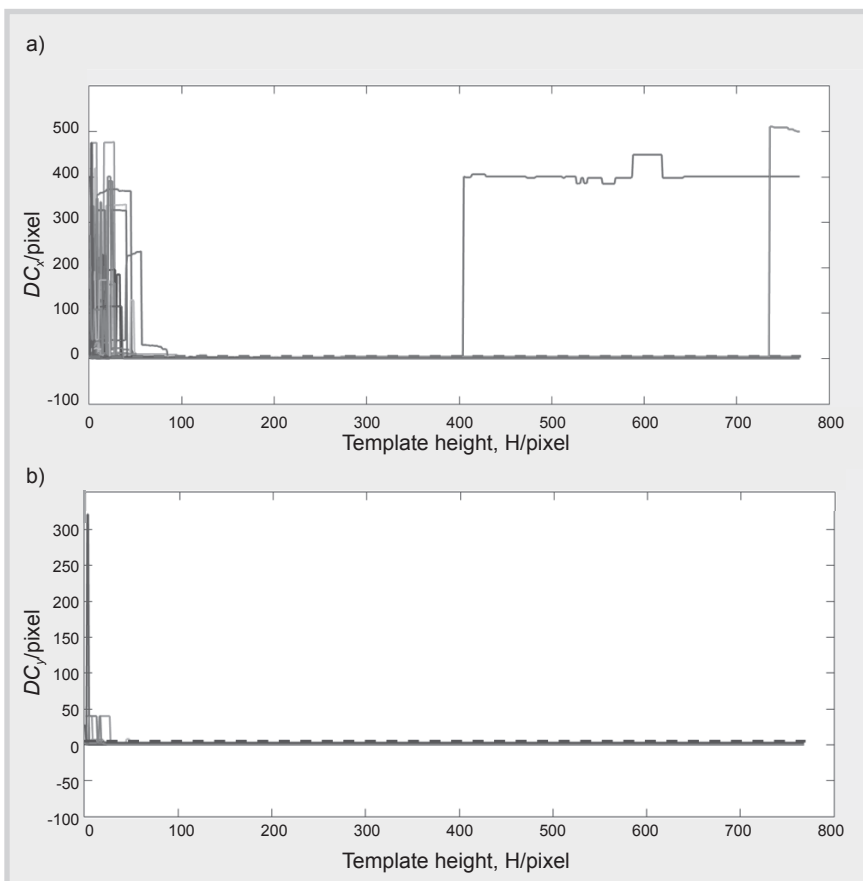


Figure 7. Two DC value results of 100 image pairs at different H values: a) DC_x & b) DC_y .

es. In order to avoid a negative value, u_p values are shown in **Figure 6.b**, in which the difference between the two methods is close when H is small, and with an increase in H , the u_p values are constant. It can also be seen that the distance between the two methods is 2-3 pixels, and thus it can be accepted.

From the single image pair, we cannot determine the optimal H . Thus the u_p values and MC values of 100 image pairs are measured further to ensure the optimal H . To observe the deviation degree of u_p values and MC values for the two methods in 100 image pairs directly, two distance curvilinear DC are drawn as defined in **Equations (6)** and **(7)**, and shown **Figure 7**.

$$DC_x = |u_p^A - u_p^M| \quad (6)$$

$$DC_y = |MC^A - MC^M| \quad (7)$$

Where u_p^A , u_p^M and MC^A , MC^M are the u_p values and MC values of the automatic method proposed and manual method, respectively.

In **Figure 7**, the dot lines represent DC values equal to 5 pixels, with the other solid lines denoting the DC values of 100 image pairs. From **Figure 7.b**, we can see that there are many large variations in the DC_y values when $H < 100$. Subsequently the data remain constant, which means that a large range of the template height can be used to measure the MC values. However, there is a mutate value when H equals about 400 pixels in **Figure 7.a**. Therefore it can be concluded that the deviation distance of u_p and MC testing for the two methods is less than 5 pixels as H changes in the interval $[100, 400]$. Since the computation time is related to the number of data in the matching template, the larger the template height H is, the longer the computation time. Hence the optimal size of the matching template is $100 \times N$ pixels.

Threshold values

In the automatic image mosaic method, an easy threshold value T_1 is set to get the first binary image which has clear hairiness. Then another threshold T_2 is applied to segment the original image to obtain a second binary image which has little hairiness. Subsequently the little hairiness is removed from the second binary image with two judgment templates. There are two threshold values

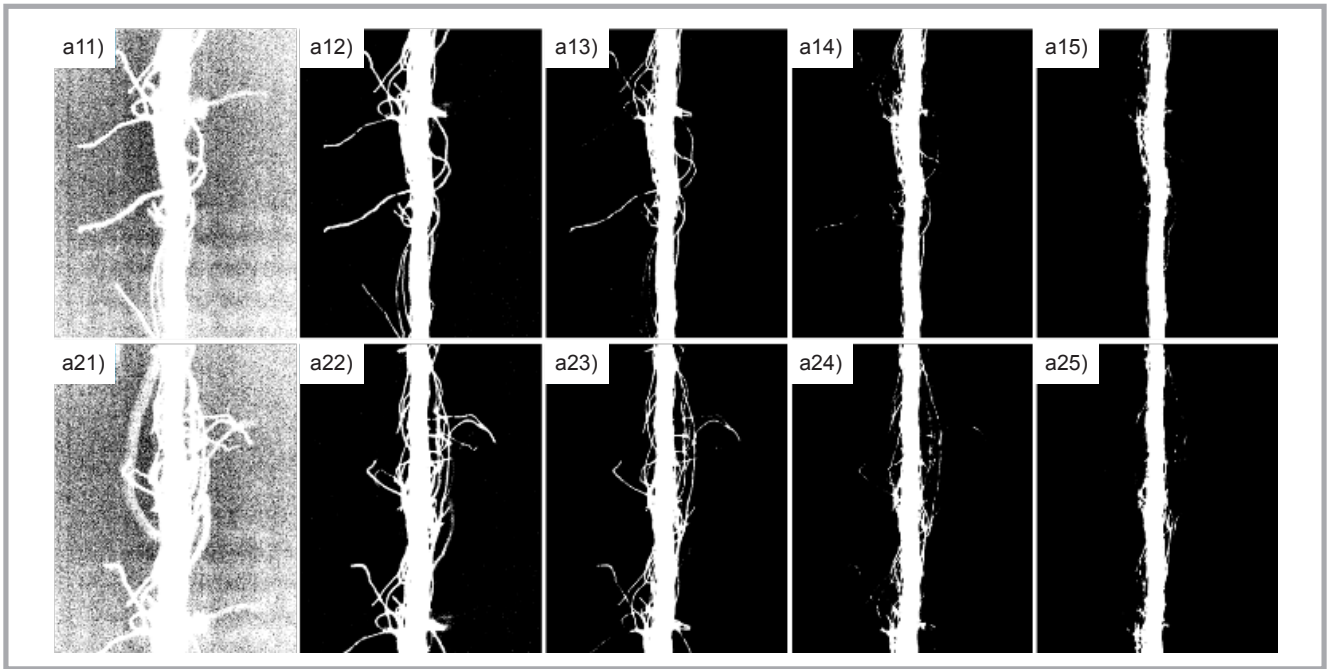


Figure 8. Different segmentation results with different T_1 values: a11)-a21) 0, a12)-a22) 20, a13)-a23) 40; a14)-a24) 60; a15)-a25) 80.

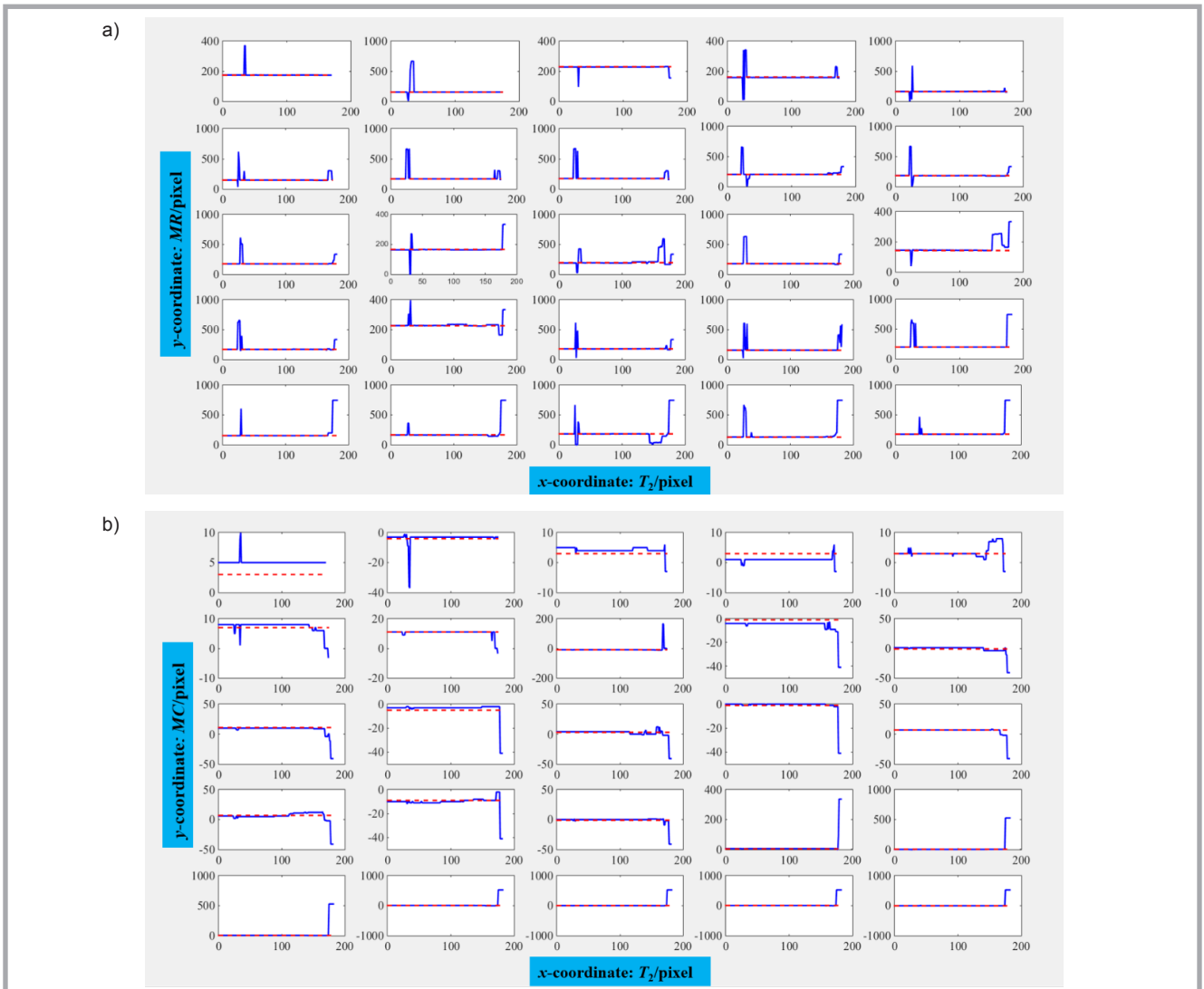


Figure 9. MR and MC measurement results at different T_2 values based on the two methods inspected: a) MR measurement results, b) MC measurement results.

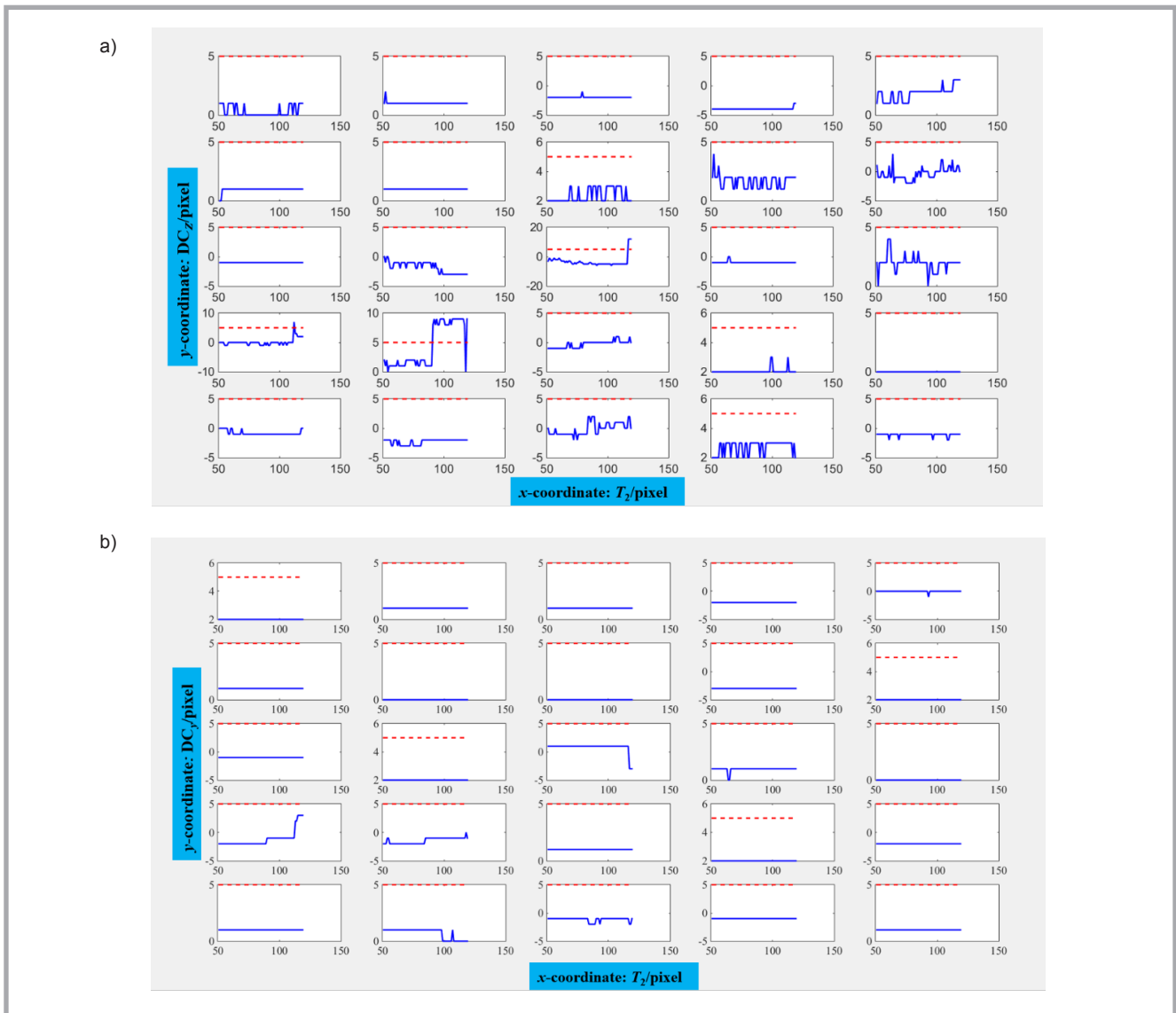


Figure 10. DC_z and DC_y curves as $T_2 \in [51, 119]$: a) DC_z curves, b) DC_y curves.

that need to be discussed to determine their impact on the matching precision. Due to the first binary image needing to contain more hairiness, the second binary image needs to contain less hairiness, and the template image cannot be a zero matrix; the values of T_1 and T_2 can only be a small part of the range from 0 to 255. In order to avoid unnecessary parameter discussion, the range of T_1 can be determined first. Take Figures 2.a1 and 2.a2 as an example, the different segmentation results with varying T_1 are shown in Figure 8.

From Figure 8, it can be seen that the level of hairiness in the segmentation images decreases as the T_1 value increases, and more hairiness can be obtained when $T_1 \leq 40$. Long hairiness information is almost removed when $T_1 = 60$ in two yarn images, and the discussion will be

meaningless if the first binary image does not contain more hairiness detail. Hence the initial scope of T_1 can be set as $[0, 40]$. From Figure 8, we can also see that there are much background noise when $T_1 < 20$. This can produce a certain effect on the accuracy of automatic image matching. Finally the range of $[20, 40]$ can be used to segment the yarn image which has clear hairiness. Moreover the selection of T_1 in the interval $[20, 40]$ has little impact on the selection of T_2 and the stitching results. Therefore, T_1 is set as 30 in the following discussion.

In order to determine the optimum scope of T_2 , 100 image pairs of #1 yarn at a 40 fps frame rate, $T_1 = 30$, and $100 \times N$ pixel template size were measured as T_2 changes in the interval $[0, 255]$. MR and MC detection results of 25 image pairs are shown in Figure 9.

In Figure 9, the red dot lines represent measurement results of the manual method at different T_2 values, and the blue solid lines denote the results of the automatic method with $T_1 = 30$ and T_2 changing from 0 to 255. From Figure 9.a, it can be found that there are two big changes (having quite a distance from the red dotted line) in MR measurement. These two big changes vacillate in the interval of $T_2 \in [20, 50]$ and $[120, 255]$. In MC measurement, the automatic method shows a big difference from the manual method when $T_2 \in [130, 200]$. Combining these unusual intervals, the optimal range of T_2 can probably be determined as $[0, 19]$ and $[51, 119]$. This means that the result detected will be accurate when the threshold value is $T_2 \in [0, 19] \cup [51, 119]$.

In the image processing, a second binary image with little hairiness is required.

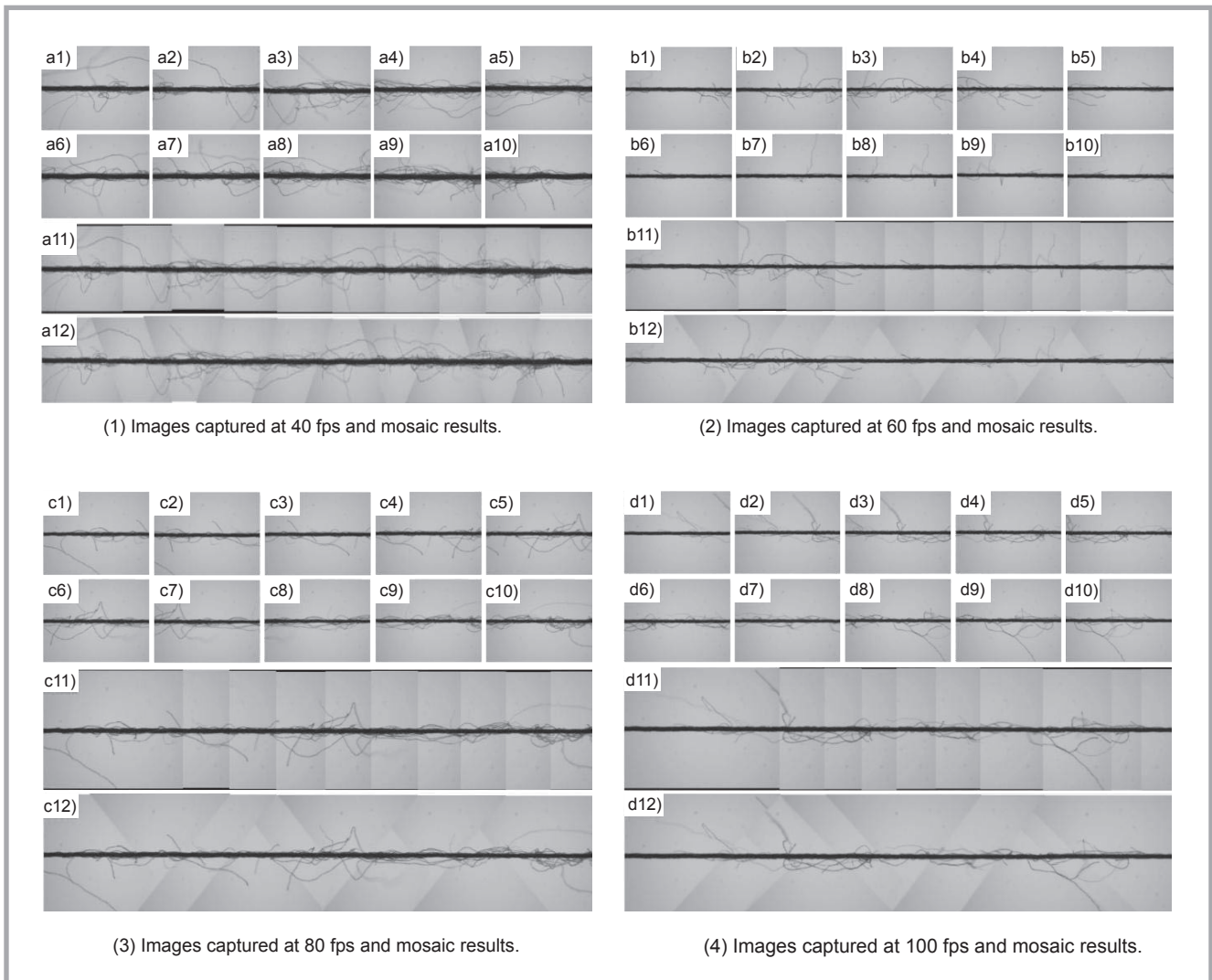


Figure 11. The consecutive yarn images captured at different frame rates and their panoramic images stitched by the two methods: a1)-d1) tenth image, a2)-d2) ninth image, a3)-d3) eighth image, a4)-d4) seventh image, a5)-d5) sixth image, a6)-d6) fifth image, a7)-d7) fourth image, a8)-d8) third image, a9)-d9) second image, a10)-d10) first image, a11)-d11) stitching result images by the automatic method proposed, and a12)-d12) stitching result images by the manual method.

However, the second binary image will contain more hairiness when T_2 is a small value. The computation time will increase significantly when using the judge template method to remove yarn hairiness. Thus the optimum interval of T_2 can be set as [51, 119]. To observe the deviation degree of MR and MC results for the two methods directly as T_2 changes from 51 to 119, distance curvilinear DC_y and DC_z are drawn in **Figure 10**. DC_z is defined as:

$$DC_z = |MR^A - MR^M| \quad (8)$$

where, MR^A & MR^M are MR values of the automatic method proposed and manual method, respectively.

In **Figure 10**, the red dotted lines represent DC_y values equal to 5 pixels. In **Figure 10.b**, all the DC_y values are less than 5 pixels. However, some DC_z values

are greater than 5 pixels in **Figure 10.a**, such as the sub-figure located at line 3 column 3, line 4 column 1 and line 4 column 2. From these sub-figures, we can see that some DC values are greater than 5 pixels when $T_2 > 85$. Thus the range of T_2 can be further narrowed. After analysing all the image pairs of three kinds of slub yarn, the range of T_2 is determined as [51, 80].

Different frame rate

In the pre-work phase, the images captured at 40 fps were measured to detect the accuracy of matching position information. In the above section, a template size of $100 \times N$ pixels is selected as the optimal. Hence the overlapping parts of neighbouring images must be greater than 100 pixels. Due to the frame rate being unstable in the process of image capture, the minimum frame rate is set

as 40 fps to maximally avoid detection errors at a yarn speed of 6 m/min. In this section, 100 image pairs of three kinds of slub yarn acquired at 40, 60, 80, and 100 fps were measured by the manual method and automatic method proposed. A panoramic image matching row MR and matching column MC was obtained at a template size of $100 \times N$ pixels, $T_1 = 30$, and $T_2 = 60$. The panoramic images, which are stitched by the automatic method and manual method based on 10 consecutive yarn images of yarn #1 captured at 40, 60, 80, and 100 fps, are shown in **Figure 11**.

From the stitching result images, we can see that the proposed method results agree well with those of the manual method at different frame rates. The results of the two detection methods are visibly the same. To objectively evaluate the quali-

Table 2. Mosaic results of two methods at 40 and 60 fps based on nine yarn image pairs. **Note:** *A* – denotes the automatic method proposed; *M* – denotes the manual method.

x-th image pair	40 fps						60 fps					
	MR		E_{MR} %	MC		E_{MC} %	MR		E_{MR} %	MC		E_{MC} %
	A	M		A	M		A	M		A	M	
1	174	174	0.00	5	3	0.33	354	354	0.00	-3	0	0.50
2	155	154	0.13	-3	-4	0.17	353	350	0.39	4	3	0.17
3	228	230	0.26	4	3	0.17	341	342	0.13	-1	-1	0.00
4	158	162	0.52	1	3	0.33	336	338	0.26	2	3	0.17
5	164	162	0.26	3	3	0.00	330	330	0.00	-1	-1	0.00
6	147	146	0.13	8	7	0.17	334	334	0.00	2	3	0.17
7	167	166	0.13	11	11	0.00	331	330	0.13	2	3	0.17
8	173	170	0.39	-9	-9	0.00	336	338	0.26	3	3	0.00
9	203	202	0.13	-4	-1	0.50	344	342	0.26	-2	-1	0.17

Table 3. Mosaic results of two methods at 80 and 100 fps based on nine yarn image pairs. **Note:** *A* – denotes the automatic method proposed; *M* – denotes the manual method.

x-th image pair	80 fps						100 fps					
	MR		E_{MR} %	MC		E_{MC} %	MR		E_{MR} %	MC		E_{MC} %
	A	M		A	M		A	M		A	M	
1	439	438	0.13	-2	0	0.33	518	518	0.00	-1	0	0.17
2	422	422	0.00	2	3	0.17	521	526	0.65	1	0	0.17
3	420	422	0.26	0	-1	0.17	327	330	0.39	4	3	0.17
4	430	430	0.00	2	3	0.17	359	354	0.65	3	3	0.00
5	411	414	0.39	-1	-1	0.00	447	446	0.13	-2	-1	0.17
6	418	418	0.00	-2	-1	0.17	475	474	0.13	-4	-5	0.17
7	396	398	0.26	4	3	0.17	496	498	0.26	3	3	0.00
8	409	410	0.13	6	7	0.17	484	482	0.26	-1	-1	0.00
9	413	414	0.13	-4	-5	0.17	446	446	0.00	6	7	0.17

ties of the image mosaic, *MR* and *MC* results of the two methods at 40, 60, 80 and 100 fps based on ten consecutive yarn images are list in **Tables 2** and **3**.

In **Tables 2** and **3**, E_{MR} and E_{MC} represent the relative error of the image mosaic in the vertical and horizontal directions, as defined in **Equations (9)**, **(10)**. *M* is the height of the image and *N* the width. Here, $M = 768$, $N = 600$.

$$E_{MR} = \left| \frac{DC_z}{M} \right| \times 100\% \quad (9)$$

$$E_{MC} = \left| \frac{DC_y}{N} \right| \times 100\% \quad (10)$$

From **Tables 2** and **3**, it can be seen that the automatic mosaic method proposed can get good results at 40, 60, 80 and 100 fps from the nine image pairs. The values of E_{MR} are less than 0.52%, 0.39%, 0.39% and 0.65% at four frame rates, respectively, and E_{MC} are less than 0.5%, 0.5%, 0.33%, and 0.17%. It means that the error in *MR* and *MC* for the two methods is no more than 5 pixels, which can be considered acceptable.

To evaluate the mosaic result further, the *MR*, *MC*, DC_z and DC_y results of all 100 yarn image pairs (101 images) of yarns #1, #2 and #3 at four frame rates

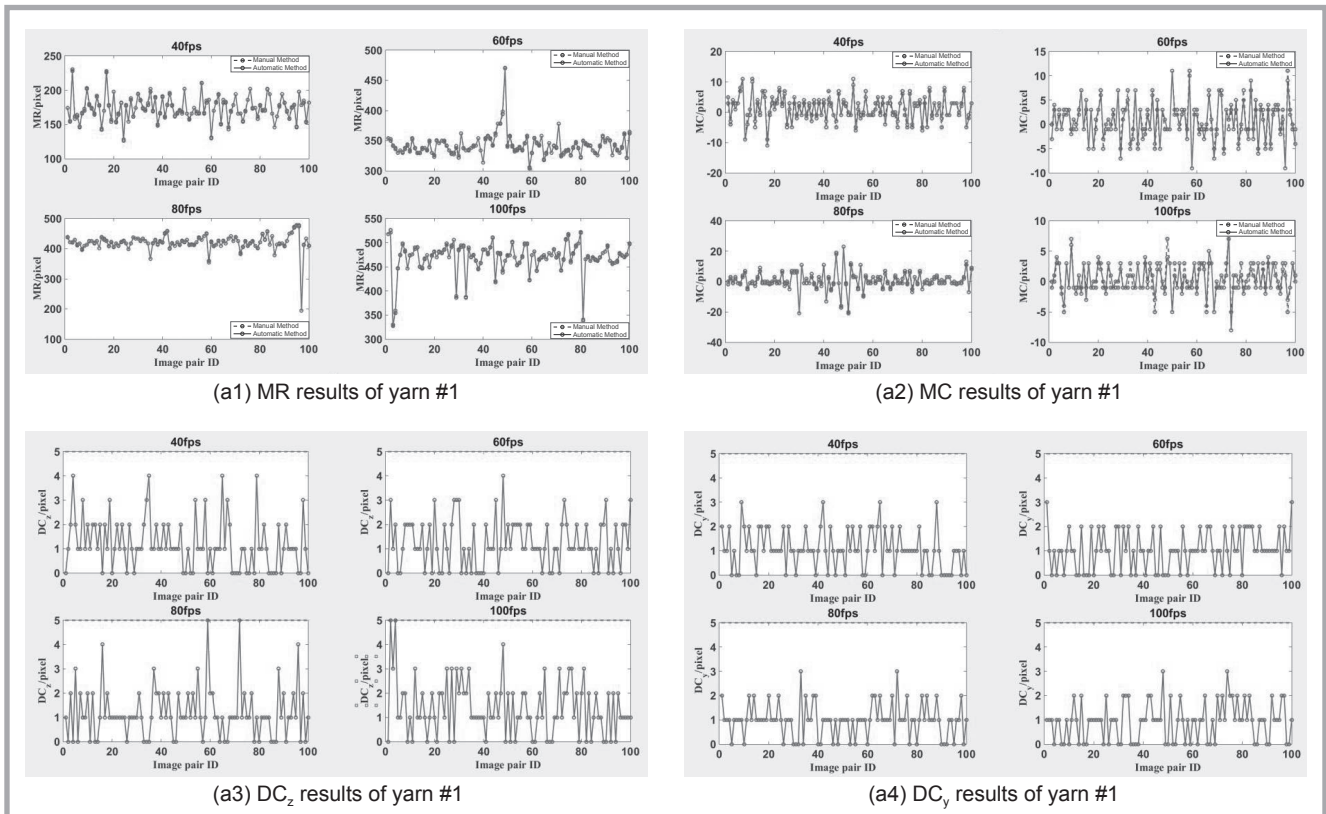


Figure 12. Testing results of three kinds of yarn at four frame rates based on two measurement methods: (a1)-(a4) measuring results of yarn #1.

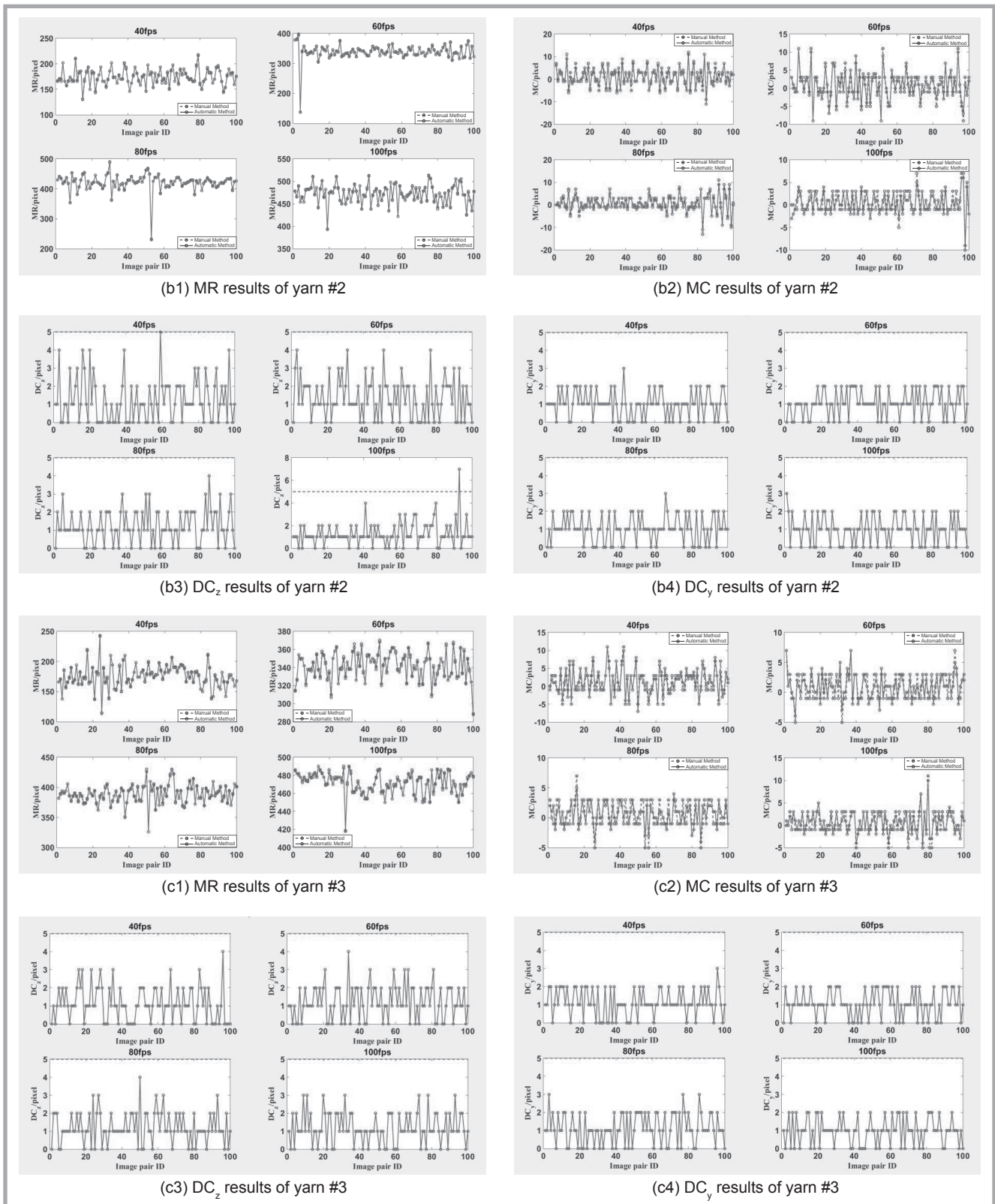


Figure 12. Testing results of three kinds of yarn at four frame rates based on two measurement methods: (b1)-(b4) measuring results of yarn #2, (c1)-(c4) measuring results of yarn #3.

Table 4. Comparison of time taken using the automatic method proposed and the manual method at four frame rates based on 100 image pairs.

	#1				#2				#3			
	40	60	80	100	40	60	80	100	40	60	80	100
Automatic/s	32.1	31.9	29.6	32.0	31.7	32.7	32.8	32.7	34.1	33.3	33.5	33.2
Manual/min	>37.8	>39.2	>36.5	>39.1	>38.2	>37.6	>40.1	>38.4	>39.5	>40.2	>37.9	>41.3

for the two measurement methods are shown in *Figure 12*.

In *Figures 12.a1-12.c1* and *12.a2-12.c2*, the dashed line denotes *MR* and *MC* results of the manual method, and the solid lines represent the results of the automatic method proposed. In *Figures 12.a3-12.c3* and *12.a4-12.c4*, the dashed lines represent *DC* values equal to 5 pixels, and the other solid represent lines *DC* values of 100 image pairs. From these figures, it can be seen that the *MR* and *MC* results are about the same for the two testing methods at the four frame rates. The DC_x and DC_y results are all less than 5 pixels. Therefore the automatic method proposed for stitching the sequence yarn image is effective.

Computing time analysis

A comparison of the time taken using the automatic method proposed and the manual method at the four frame rates based on 100 image pairs is shown in *Table 4*. In the manual method, it takes more than 37 minutes to stitch 101 images into panorama ones. In the computer method proposed, it takes less than 35 seconds for the image mosaic. It is also noted that the time for the image mosaic includes the image segmentation time. All the implementations were done in MATLAB on a Lenovo G480a with 2.6 GHz processor, 4 GB RAM. The computational time is measured in “seconds”. Therefore the overall processing time of the approach proposed is greatly shorter than that of the approach in the manual method, and when there are more source images captured as input of panorama stitching, the amount of time saved by the parallel executing feature of the approach proposed is more significant.

Conclusions

In an earlier work, an effective method for stitching sequence slub yarn images automatically was developed based on image processing and the NCC method. 100 image pairs of two kinds of slub yarn were measured in certain specific conditions, and the measurement results were evaluated with the manual method. In this paper, experiments were carried out to investigate the feasibility and accuracy of the method proposed for the automatic mosaic of sequence slub yarn images. Three 100% cotton yarns of 27.8, 15.6, and 9.7 tex were prepared and used for evaluation.

In the experiment, the optimum template size and threshold values were determined first based on the experimental data. Then the detection results at different frame rates and the optimum parameters were analysed to evaluate the accuracy of image stitching. The computing time was also assessed at different frame rates for the automatic method proposed and the manual method.

The experimental results show that the method proposed can accurately find the stitch position and have a high consistency with the manual method when the matching template is $100 \times N$ pixels, the threshold value $T_1 \in [20, 40]$ and $T_2 \in [51, 80]$, and when the frame rate is greater than 40 fps. Using all these optimum parameters, the geometric parameters of slub yarn can be measured precisely.

Acknowledgements

The authors would like to acknowledge the Research Innovation Program for College Graduates of Jiangsu Province (Grant No. KYLX_1132), Postdoctoral Project (1601017A), and Fundamental Research Funds for the Central Universities (No. JUS-RP51631A).

References

1. Liu J, Xie Z, Gao W, Jiang H. Automatic Determination of Slub Yarn Geometrical Parameters Based on an Amended Similarity-based Clustering Method. *Textile Research Journal* 2010; 80:1075-1082.
2. Wang J, Huang X. Parameters of Rotor Spun Slub Yarn. *Textile Research Journal* 2002; 72: 12-16.
3. Barella A. Law of Critical Yarn Diameter and Twist Influence on Yarn Characteristics. *Textile Research Journal* 1950; 20: 249-258.
4. Baghernezhad S, Ghane M, Moezzi M. Strain monitoring in woven fabrics with locally induced mass irregularities using an image based method. *FIBRES & TEXTILES in Eastern Europe* 2016; 24, 2(116): 73-80. DOI: 10.5604/12303666.1191430.
5. Wray GR. The Properties of Air-Textured Continuous Filament Yarns. *Journal of the Textile Institute* 1969; 60: 102-126.
6. Yousefzadeh-Chimeh M, Amani-Tehran M, Latifi M, Mohaddes-Mojtahedi MR. Characterizing Bulkiness and Hairiness of Air-Jet Textured Yarn Using Imaging Techniques. *Journal of the Textile Institute* 2005; 96: 251-255.
7. Elkhalek RA, Elbealy R, Eldeeb A. A Computer-Based System for Evaluation of Slub Yarn Characteristics. *Journal of Textiles* 2014; 1:1-11.

8. Liu J, Li Z, Lu Y, Jiang H. Visualization and determination of the geometrical parameters of slub yarn. *FIBRES & TEXTILES in Eastern Europe* 2010; 18, 1(78): 31-35.
9. Pan R, Gao W, Liu J, Wang H. Recognition the parameters of slub-yarn based on image analysis. *Journal of Engineered Fibers and Fabrics* 2011; 6: 25-30.
10. Liu X., Wen Z, and Su, Z. Slub Extraction in Woven Fabric Images Using Gabor Filters. *Textile Research Journal* 2008; 78: 320-325.
11. Juan L and Gwun O. SURF applied in panorama image stitching. In: *2010 2nd international conference on image processing theory, tools and applications*. Paris, 7-10 July 2010, pp.495-499.
12. Li YF, Wang YM, Huang WQ, Zhang Z. Automatic image stitching using SIFT. In: *International conference on audio, language and image processing*. Shanghai, 7-9 July 2008, pp.568-571.
13. Yang F, Wei LL, Zhang ZW, et al. Image mosaic based on phase correlation and Harris operator. *Journal of Computer Information Systems* 2012; 8: 2647-2655.
14. Bouwmans T. Recent advanced statistical background modeling for foreground detection: a systematic survey. *Recent Patents on Computer Science* 2011; 4: 147-176.
15. Brown M, Lowe D. Recognising panorama. In: *Proceedings of international conference on computer vision* 2003. p. 1218-1225.
16. Li SY, Xu BG, Tao XM, Chi ZR. An intelligent computer method for automatic mosaic and segmentation of tracer fiber images for yarn structure analysis. *Textile Research Journal* 2014; 85:733-750.
17. Li Z, Xiong N, Wang J, Pan R, Gao W, Zhang N. An intelligent computer method for automatic mosaic of sequential slub yarn images based on image processing (Accept).
18. Li, ZJ, Pan, RR, Zhang J, Li BB, Gao WD, Bao W. Measuring the unevenness of yarn apparent diameter from yarn sequence images. *Measurement Science & Technology* 2016; 27: 015404.
19. Li Z, Pan R, Wang J, Wang Z, Li B, Gao W. Real-time Segmentation of Yarn Images Based on an FCM Algorithm and Intensity Gradient Analysis. *FIBRES & TEXTILES in Eastern Europe* 2016; 24, 4(118): 45-50 DOI: 10.5604/12303666.1201130.
20. Lewis JP. Fast Normalized Cross-Correlation. *Circuits Systems & Signal Processing* 2001; 82: 144-156.
21. Russ JC. Template matching and correlation, in: *The Image Processing Handbook*, 2 ed., CRC Press, Raleigh, 1994; p. 341-346.
22. Hii AJH, Hann CE, Chase JG, Houten EEVW. Fast normalized cross correlation for motion tracking using basis functions. *Computer Methods & Programs in Biomedicine* 2006; 82: 144-156.

Received 29.09.2017 Reviewed 23.11.2017